Biochemical and Biophysical Research Communications 450 (2014) 844–850

Contents lists available at ScienceDirect

Biochemical and Biophysical Research Communications

journal homepage: www.elsevier.com/locate/ybbrc

Monocyte to macrophage differentiation-associated (MMD) targeted by miR-140-5p regulates tumor growth in non-small cell lung cancer

Weina Li [a,1,*], Fei He [b,1,2]

[a] Department of Biomedical Engineering, Fourth Military Medical University, Xi'an 710032, China
[b] Department of Hepatic Surgery, Xijing Hospital, Fourth Military Medical University, Xi'an 710032, China

ARTICLE INFO

Article history:
Received 13 June 2014
Available online 24 June 2014

Keywords:
Lung cancer
MMD
MicroRNA
Cell proliferation

ABSTRACT

Monocyte to macrophage differentiation-associated (MMD) is identified in macrophages as a gene associated with the differentiation from monocytes to macrophages. Recent microarray analysis for non-small cell lung cancer (NSCLC) suggests that MMD is an important signature associated with relapse and survival among patients with NSCLC. Therefore, we speculate that MMD likely plays a role in lung cancer. In this study, we found that the protein level of MMD was increased in lung cancer compared to benign lung tissues, and knockdown of MMD inhibited the growth of A549 and Lewis lung cancer cells (LLC) *in vitro* and *in vivo*. Integrated analysis demonstrated that MMD was a direct functional target of miR-140-5p. Furthermore, we found that miR-140-5p/MMD axis could affect the cell proliferation of lung cancer cells by regulating Erk signaling. Together, our results highlight the significance of miR-140-5p/MMD axis in lung cancer, and miR-140-5p/MMD axis could serve as new molecular targets for the therapy against lung cancer.

1. Introduction

Lung cancer, predominantly non-small cell lung cancer (NSCLC) is the most common cancer and is the leading cause of cancer-related mortality in the worldwide [1]. Despite recent advances in the diagnosis and treatment of cancer, the 5-year overall survival rate associated with NSCLC is only 11% [2]. Therefore, an in-depth understanding of the molecular mechanisms underlying NSCLC development and progression is urgently needed.

Recently, the gene expression profile was evaluated and a five-gene signature was reported to be prognostic for relapse and survival in patients with NSCLC [3]. The five genes included dual specificity phosphatase 6 (*DUSP6*), monocyte to macrophage differentiation-associated (*MMD*), signal transducer and activator of transcription 1 (*STAT1*), v-erb-b2 erythroblastic leukemia viral oncogene homolog 3 (*ERBB3*), and lymphocyte-specific protein tyrosine kinase (*LCK*). The identification of five genes that can predict the clinical outcome in patients with NSCLC may reveal targets for the development of therapy for lung cancer. Among the five genes, we focus on the *MMD*. MMD is preferentially expressed in mature macrophages [4], and further studies demonstrate that MMD is implicated in macrophage activation [5]. However, MMD mRNA can be detected in almost all tissues [5] and its function is still little understood in lung cancer. Here, we found that the protein level of MMD was increased in lung cancer tissues, and knockdown of MMD could inhibit the growth of A549 and Lewis lung cancer cells (LLC).

MicroRNAs are a class of small non-coding RNA molecules that can regulate the expression of protein-coding genes at the post-transcriptional level through imperfect base pairing with the 3′-untranslated region (3′-UTR) of target mRNAs [6]. Recently, accumulating evidence indicates that microRNAs can function as oncogenes or tumor suppressors in a variety of cancers, including lung cancer [7,8]. In this study, we demonstrated that MMD was the target of a tumor-suppressing microRNA, miR-140-5p [9–12], and miR-140-5p/MMD axis played an important role in the proliferation of A549 and LLC cells. Our findings suggest miR-140-5p/MMD may serve as a novel molecular target for the development of new agents for lung cancer therapy.

2. Materials and methods

2.1. Patient samples

Paired NSCLC and adjacent non-tumorous lung tissues were obtained from 22 patients at Tangdu Hospital (Xi'an, China). The

* Corresponding author. Fax: +86 29 84774834.
E-mail addresses: liweina228@163.com (W. Li), hesili1027@163.com (F. He).
[1] These authors contributed equally to this study.
[2] Fax: +86 29 83246270.

http://dx.doi.org/10.1016/j.bbrc.2014.06.075
0006-291X/

use of clinical samples in this study was approved by the Tangdu Hospital Ethic Committee in Fourth Military Medical University. The clinicopathological characteristics of the NSCLC patients are summarized in Supplementary Table S1.

2.2. Histology and immunohistochemistry

Formaldehyde-fixed lung tissues and lung cancer tissues were paraffin-embedded, sectioned at 5 μm thickness, and were stained with hematoxylin–eosin (H&E) according to routine protocols. The levels of MMD were assessed by immunohistochemistry following the standard protocols. Tissue sections were stained with rabbit anti-MMD as primary antibody (1:100 dilution; reference 13, gifted from Professor Chen) and then incubated with horseradish peroxidase (HRP)-labeled goat anti-rabbit IgG antibody (1:100 dilution; Boster Bio Tec, Wuhan, China). These sections were visualized with DAB kit (Zhongshan Golden Bridge Bio-technology, Beijing, China). Images were taken under a microscope (Olympus BX51, Tokyo, Japan) with a CCD camera (Olympus DP70, Tokyo, Japan).

2.3. Cell culture and transfection

The lung cancer cell line A549 or LLC was cultured with DMEM (Invitrogen, Carlsbad, CA, USA) supplemented with 10% fetal bovine serum, 100 μg/ml streptomycin and 100 U/ml penicillin. MiR-140-5p mimics, the negative control of mimics, miR-140-5p inhibitor, or the negative control of inhibitor (100 nM, Ribo bio, Guangzhou, China) was transfected into A549 or LLC cells using Lipofectamine 2000 (Invitrogen) according to the manufacturer's protocol.

2.4. Lentivirus infection and selection

pLKO-shMMD-1, pLKO-shMMD-2 and pLKO-shm-MMD were constructed by inserting a short hairpin double-stranded oligonucleotide targeting MMD into pLKO.1 (Addgene, Cambridge, MA, USA). The sequences of shMMD-1, shMMD-2 and shm-MMD oligonucleotides are listed in Supplementary Table S2. Viral particles were prepared by transfection of HEK293T cells with three plasmids: shRNA vector/psPAX2/pMD2.G (Addgene), according to the recommended protocols. A549 or LLC cells were transduced with the medium containing lentiviral particles. Cells were selected with 2 μg/ml puromycin at 48 h post-infection. And the knockdown of MMD was monitored by Western blot analysis.

2.5. Cell cycle analysis

A549 or LLC cells were harvested, and fixed with 70% ethanol at room temperature for 20 min. Then cells were washed and resuspended in PBS containing 50 μg/ml of propidium iodide, 0.1 mg/ml RNase A and 0.1% Triton X-100 for 10 min, and cell cycle was analyzed using a FACSCalibur™ (BD Biosciences, San Jose, CA, USA). Data analysis was performed using the CellQuest software (BD Biosciences).

2.6. MTT assay

Cells were plated in 96-well plates at 1000 cells per well in 200 μl of the medium. Cell growth was assayed every day for 5 days, by adding 20 μl MTT (5 mg/ml) solution. Cells were incubated further at 37 °C for 4 h, and then aspired the medium and 150 μl of dimethyl sulfoxide (Sigma, Saint Louis, MO, USA) was added to each well, followed by mixing at room temperature for 10 min. The absorbance of the supernatant was measured at 492 nm.

2.7. Tumor-bearing mouse model

A549 cells or LLC (5×10^6) were injected subcutaneously into nude mice or B6/C57 mice brought about under specific pathogen-free conditions. Nine to ten days after the initial inoculation, tumor growth was monitored every 2–3 days by measuring tumor length (L) and short (S) with a sliding caliper. Tumor size was calculated as $L \times S^2 \times 0.51$. Eighteen days after the initial inoculation, A549 tumors were removed and measured. Twenty-one days after the initial inoculation, LLC tumors were removed and measured. All animal experiments were approved by the Animal Experiment Administration Committee of the Fourth Military Medical University.

2.8. Prediction of microRNAs targeting MMD

The microRNAs targeting MMD mRNA were predicted using four different prediction programs: TargetScan (http://www.targetscan.org), PicTar (http://pictar.mdc-berlin.de/cgi-bin/new_PicTar_vertebrate.cgi), microrna (http://www.microrna.org/microrna/getGeneForm.do) and miRDB (http://mirdb.org/miRDB). Only the miRNAs predicted by all four algorithms were considered to be putative regulators of MMD and were selected for further experimental identification.

2.9. Quantitative real-time reverse-transcription PCR

Total RNA was prepared using Trizol reagent (Invitrogen) according to the manufacturer's instructions. Complementary DNA was prepared using PrimerScript RT Reagent Kit (Takara, Dalian, China). Quantitative Real-time PCR was performed using SYBR Premix EX Taq™ II Perfect Real time kit (Takara, Dalian, China) and the ABI PRISM 7500 real-time PCR system, with human β-actin as an internal control. The primers for qPCR are listed in Supplementary Table S2. For the detection of microRNAs, microRNA purification kit, reverse-transcription kit, RT-PCR microRNAs Detection kit and RT-PCR Primer Sets purchased from QIAGEN (Hilden, Germany). Expression of U6 was used as an internal control.

2.10. Reporter assay

For 3′-UTR reporter assay, the 3′-UTR of MMD (1721 bp) was amplified by PCR from human genomic DNA. The resulting fragment was inserted into pGL3-promoter (Promega, Madison, WI, USA), to generate a reporter construct MMD-3′-UTR. We also mutated complementary seed sequences in the miR-140-5p–binding region (ACCACT → CATATG), and generated a reporter construct MMD-3′-UTR-mut. A549 cells (2.5×10^4) were transfected with 0.1 μg of reporter construct, 100 nM of miR-140-5p mimics or negative control (NC), and 5 ng of Renilla luciferase vector (phRL-TK, Promega) using Lipofectamine 2000 (Invitrogen) according to the recommended protocol. Twenty-four hours after the transfection, luciferase activity was assessed using Luminoskan Ascent (Labsystems, Helsinki, Finland) and a Dual-Luciferase Reporter Assay Kit (Promega) according to the manufacturer's protocol. All luciferase activity was normalized to Renilla luciferase activity. The oligonucleotide sequences used for vector construction are listed in Supplementary Table S2.

2.11. Western blot

Tissue or cell protein extracts were prepared using the RIPA buffer (Beyotime, Haimen, China). The protein concentration was determined using the BCA Protein Assay reagents (Pierce, Rock, IL, USA), according to the manufacturer's instructions. The samples were analyzed by SDS-12% PAGE, blotted to PVDF membrane, and

probed using primary antibodies followed by the horseradish peroxidase (HRP)-conjugated goat anti-rabbit IgG or goat anti-mouse IgG antibodies (Boster). The primary antibodies included antibodies to MMD, Erk1/2, phosphate-Erk1/2 (Cell Signaling Tec, Boston, MA, USA), and β-actin (Sigma). The membrane was developed using the chemoluminescent reagents (Cowin Biotech, Beijing, China).

2.12. Statistic analysis

Images were imported into the Image Pro Plus 5.1 software (MediaCybernetics Inc., Bethesda, MD, USA), and positive area was analyzed. Statistical analysis was performed with the SPSS 12.0 program. Results were expressed as means ± SD. Comparisons between groups were undertaken using unpaired Student's *t*-test. MTT assay and tumor growth curve were analyzed using two-way ANOVA. And correlation between the miR-140-5p and MMD level was evaluated using Spearman's correlation coefficient. $P < 0.05$ was considered statistically significant.

3. Results

3.1. Expression of MMD is increased in lung cancer tissues

Recent studies show that MMD is closely associated with the outcomes in patients with NSCLC [3]. MMD, which is preferentially expressed in mature macrophages, may affect macrophages activation and promote the development of cancer. However, previous report demonstrates that MMD mRNA can be detected in almost all examined tissues [5]. Therefore we infer that MMD may not only play the function in macrophages, but also play a role in other cells, such as tumor cells. To clarify the function of MMD gene, we verified the expression of MMD at the protein levels in lung cancer. We initially observed the architecture of human lung cancer tissues by H&E staining. As shown in Fig. 1A, tumor tissues were condensing and nodular-like compared to paracancerous normal lung architecture. Then we detected the protein levels of MMD in lung cancers tissues and normal lung by immunohistochemistry and Western blot. As shown in Fig. 1B and C, the level of MMD was significantly increased (1.73-fold) in the nodular-like tumors compared to normal lung tissues. And we also can observe that MMD was expressed in tumor parenchyma cells. The high protein level of MMD was further confirmed by Western blot (Fig. 1D). These results indicate that MMD is highly expressed in lung cancer tissues.

3.2. Knockdown of MMD inhibits growth of A549 and LLC cells in vitro and in vivo

To investigate the function of MMD in lung cancer, we then performed loss-of-function analyses. A549 or LLC lung cancer cells were infected with lentiviral constructs containing two MMD shRNA (shMMD-1, shMMD-2 and shm-MMD) or the negative control (shScramble). Western blot analysis confirmed that the expression of MMD was suppressed by shMMD-2 and shm-MMD (Fig. 2A and Fig. S1A). Then we analyzed the cell cycle progression of the A549-shMMD-2, A549-shScramble, LLC-shm-MMD and LLC-shScramble cells. As shown in Fig. 2 B and C, Fig. S1B and C, the A549-shMMD-2 and LLC-shm-MMD cells exhibited lower proportion of cells in the G2/S phase compared with that of the control shScramble cells, suggesting that knockdown of MMD inhibited cell cycle progression of the A549 and LLC cells. Furthermore, the growth of the A549-shMMD-2 and LLC-shm-MMD cells was compared with the shScramble cells by MTT assay. As shown in Fig. 2D and Fig. S1D, the growth of the A549-shMMD-2 and

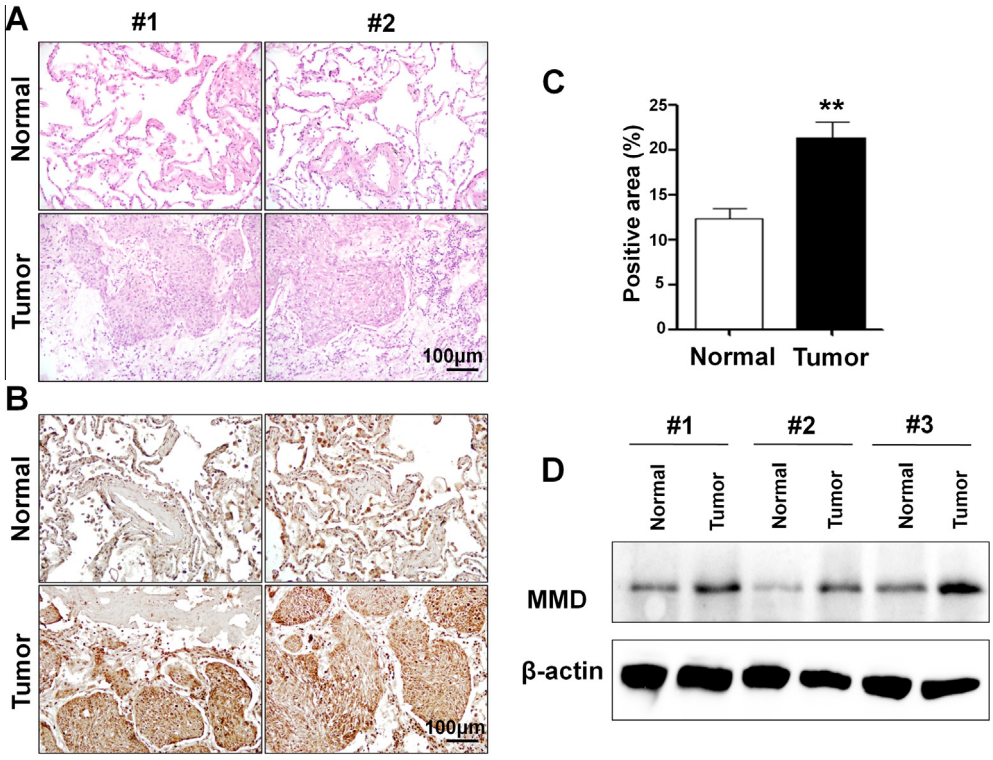

Fig. 1. MMD was up-regulated in human lung cancer tissues. (A) Two representative H&E-stained sections of the lung cancer tissues and matched normal lung tissues. (B) Immunohistochemical staining for MMD with anti-MMD in the cancerous and matched normal tissues. (C) Quantifications of the MMD-positive areas in (B) ($n = 5$). (D) Whole tissues lysates of cancerous and matched normal tissues were prepared, and the expression level of MMD was determined by Western blotting with β-actin levels as an internal control. Bars = means ± SD, $^{**}P < 0.01$.

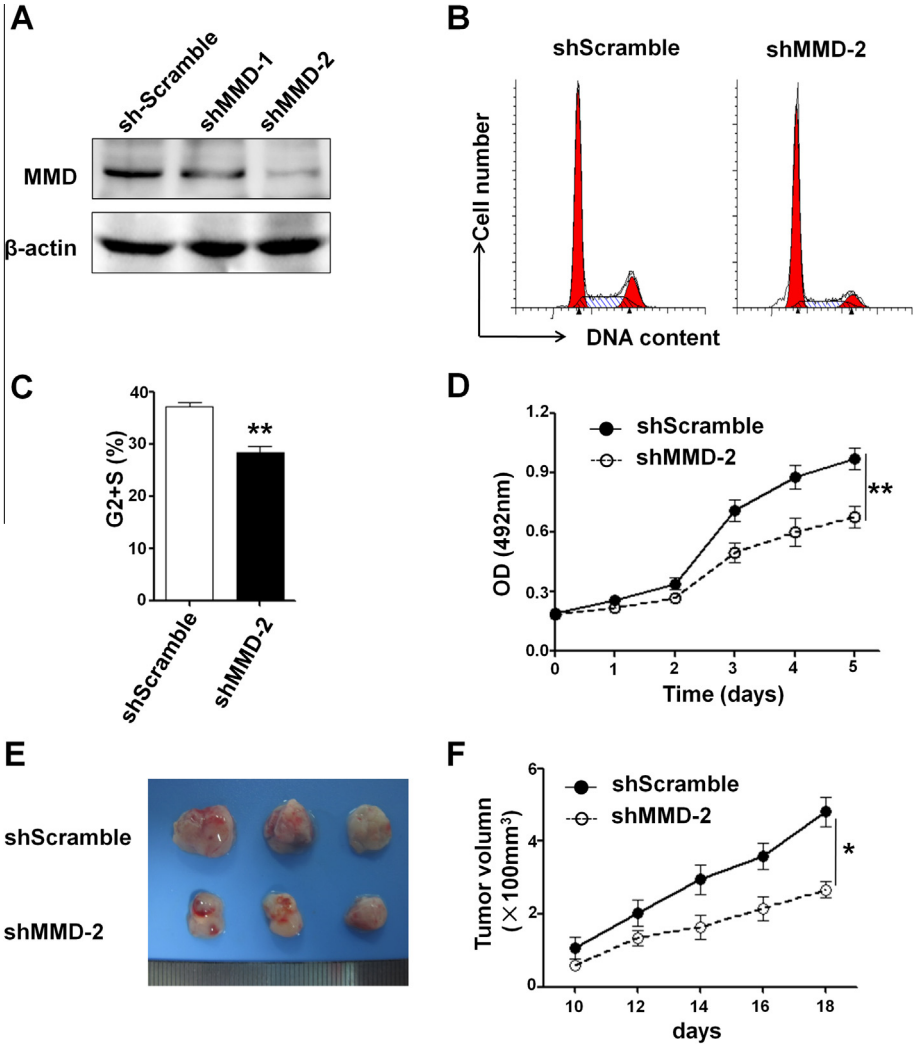

Fig. 2. Knockdown of MMD inhibited the growth of lung cancer cells *in vitro* and *in vivo*. (A) A549 cells were infected with lentivirus containing shMMD-1, shMMD-2 or shScramble, and then cells were selected with 2 μg/ml puromycin. Cell lysates were prepared and the efficiency of knockdown was monitored by Western blotting. (B and C) Cell cycle progression of A549-shScramble and A549-shMMD-2 cells was determined by FACS analysis. Then the percentage of G2/S phages was compared ($n = 5$). (D) Growth of A549-shScramble and A549-shMMD-2 was compared using the MTT assay. (E and F) A549-shScramble and A549-shMMD-2 cells were inoculated subcutaneously in nude mice. Tumor volumes were monitored every 2 days from the tenth day and were compared ($n = 6$), and representative image of tumors was shown in F. Bars = means ± SD, $^{*}P < 0.05$, $^{**}P < 0.01$.

LLC-shm-MMD cells was significantly slower than that of the shScramble cells. These results suggest that knockdown of MMD inhibits growth of lung cancer cells *in vitro*. To further determine the effect of MMD on NSCLC tumor growth *in vivo*, A549-shMMD-2 cells and A549-shScramble cells were inoculated subcutaneously into the nude mice, LLC-shm-MMD and LLC-shScramble cells were inoculated subcutaneously into the B6/C57 mice and the animals were closely monitored for tumor growth for about three weeks. The results showed that shMMD tumors were significantly smaller in size and tumor volume compared to the control tumors (Fig. 2E and F, Fig. S1E and F). Taken together, these results indicate that knockdown of MMD inhibits growth of A549 and LLC cells *in vitro* and *in vivo*, and MMD could play a role of proto-oncogene in lung cancer.

3.3. MMD is a direct functional target of miR-140-5p

Cumulating evidence has shown that microRNA plays an important role in many parts of cellular processes, including cell proliferation and tumorigenesis [6–8]. Since MMD likely affects the proliferation of lung cancer cells, we then wanted to know whether MMD could also be regulated by microRNAs. For this purpose, we predicted the possible microRNAs targeted to MMD 3′UTR with four different algorithms, the PicTar, TargetScan, microrna and miRDB. We focused our attention on miR-140-5p (Fig. 3C), which is known to suppress the growth and metastasis of NSCLC [11]. The binding site of miR-140-5p is highly conserved among vertebrates (Fig. S2). The high-degree conservation promoted us to ask whether MMD is regulated by miR-140-5p. Firstly, we analyzed the correlation of MMD and miR-140-5p in human lung cancer tissues. We used qRT-PCR to compare the expression of mature miR-140-5p and MMD mRNA in the same patient's lung cancer tissue and normal lung tissue. Then levels of miR-140-5p and MMD were counted in the form of the ratio of lung cancer to normal lung tissue. Statistical analysis of the correlation revealed a significant inverse correlation between the levels of MMD mRNA and miR-140-5p (Fig. 3A). Secondly, we found that the protein level of MMD was significantly reduced in A549 transfected with miR-140-5p mimics compared to the control (Fig. 3B). Finally, to obtain further direct evidence that MMD is a target of miR-140-5p, we investigated the binding site of miR-140-5p in the 3′-UTR of MMD mRNA (Fig. 3C). We constructed a luciferase reporter

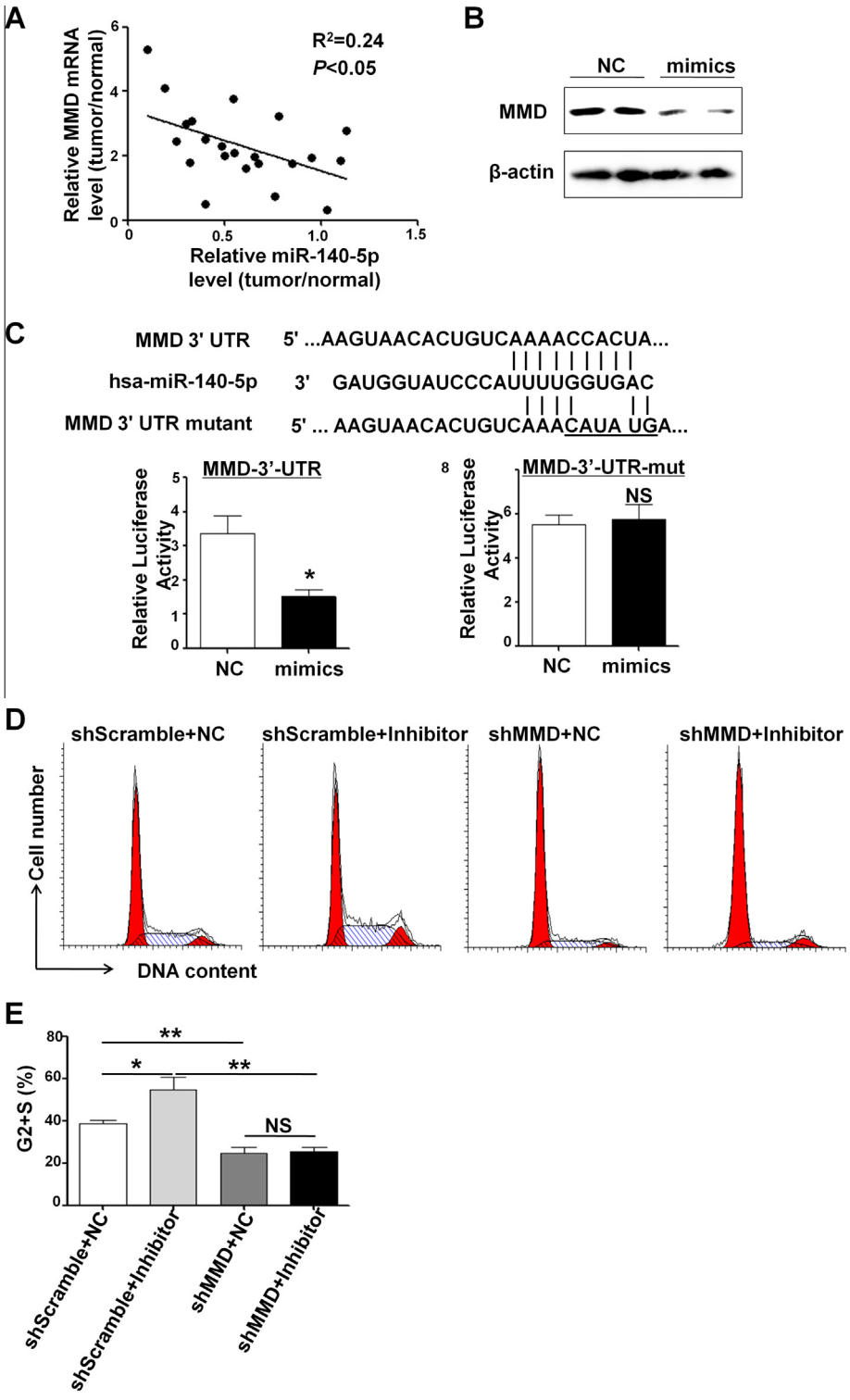

Fig. 3. MMD is a direct functional target of miR-140-5p. (A) The correlation between MMD and miR-140-5p expression in 22 pairs of NSCLC samples and matched normal lung tissues was determined using Spearman's correlation analysis. (B) A549 cells were transfected with miR-140-5p mimics (100 nM) and MMD protein levels were measured by Western blotting. (C) Sequence alignment of miR-140-5p and the MMD 3′-UTR, which contains one predicted miR-140-5p-binding site. Luciferase assay in A549 cells co-transfected with miR-140-5p mimics and a luciferase reporter containing the MMD 3′-UTR or a mutant (MMD 3′-UTR-mut). Luciferase activities were measured 24 h post-transfection. (D, E) A549-shScramble and A549-shMMD-2 cells were transfected with miR-140-5p inhibitor or negative control (100 nM), cell cycle progression was determined 48 h post-transfection. Then the percentage of G2/S phages was compared ($n = 5$). Bars = means ± SD, $^{*}P < 0.05$, $^{**}P < 0.01$.

(MMD-3′UTR) in which the nucleotides of the MMD 3′-UTR were inserted into the pGL3-promoter vector. Correspondingly, we also generated a mutant reporter (MMD-3′UTR-mut), in which the seed region was mutated. MiR-140-5p mimics or negative control were co-transfected with MMD-3′UTR or MMD-3′UTR-mut into A549 cells. The reporter assays showed that the luciferase activity in the miR-140-5p mimics group was significantly decreased compared to negative control group, and there was no effect in the

miR-140-5p and MMD-3′UTR-mut co-transfected cells (Fig. 3C). These results suggest that MMD is a direct target of miR-140-5p.

Then we wanted to know the role of miR-140-5p/MMD axis in the proliferation of lung cancer. We inhibited the level of miR-140-5p in A549 or LLC cells using its inhibitor, and found that the A549 or LLC cells transfected with miR-140-5p inhibitor exhibited higher proportion of cells in the G2/S phase compared with the A549 or LLC transfected with negative control. Furthermore, the higher proportion into cell cycle could be significantly impaired by knockdown of MMD (Fig. 3D and E, Fig. S3A and B). These results suggested that miR-140-5p/MMD axis is involved in the proliferation of A549 and LLC cells. Taken together, MMD is a direct functional target of miR-140-5p, and miR-140-5p/MMD play an important role in the proliferation of lung cancer cells.

3.4. MiR-140-5p/MMD axis regulates Erk1/2 signaling

Next we investigated the mechanisms by which miR-140-5p/MMD axis affects the proliferation of lung cancer cells. Recent studies indicate that MMD can interact with Ras and enhance its retention and activity, subsequently leading to sustain Erk signaling – an important signaling for cell proliferation [13] .Therefore, we focused on the activation of Erk1/2 in lung cancer cells. We compared the level of phosphorylated Erk1/2 in lung cancer tissues and normal lung tissues. Consistent with the higher level expression of MMD in lung cancer tissues, the phosphorylated Erk1/2 was significantly higher in tumor tissues compared to normal lung tissues (Fig. 4A). Then we depleted endogenous MMD with shRNA and examined the levels of phosphorylated Erk1/2. As shown in Fig. 4B, knockdown of MMD markedly reduced phosphorylated Erk1/2. Meanwhile, we also observed that overexpression of miR-140-5p also obviously decreased the levels of phosphorylated Erk1/2. On the other hand, we then inhibited endogenous miR-140-5p with miR-140-5p inhibitor, and found that MMD was upregulated and the phosphorylated Erk1/2 was also increased (Fig. 4C). Furthermore, the higher level of phosphorylated Erk1/2 was almost completely impaired by the knockdown of MMD (Fig. 4C). These results suggest miR-140-5p/MMD axis likely regulates the proliferation of lung cancer cells through Erk1/2 signaling.

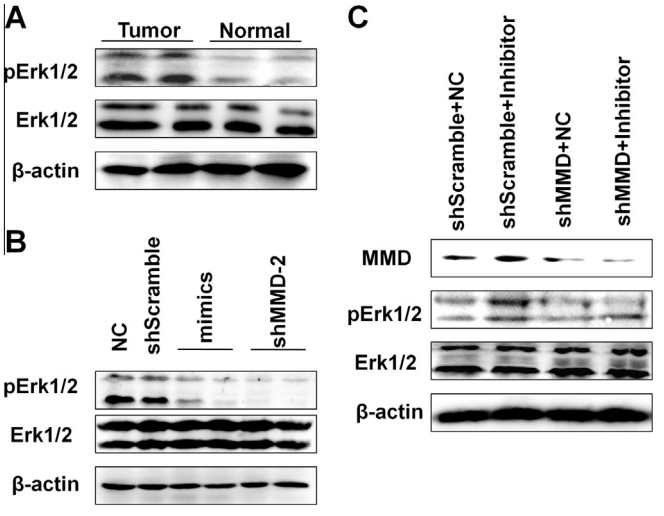

Fig. 4. MiR-140-5p/MMD axis regulates Erk1/2 signaling. (A) Whole tissues lysates of lung cancer tissues and matched normal tissues were prepared, and the level of phospho-Erk1/2 was determined by Western blotting. (B) Western blotting analysis for the level of phospho-Erk1/2 in A549-shScramble, A549-shMMD-2, A549 cells transfected with miR-140-5p mimics or negative control (100 nM). (C) A549-shScramble or A549-shMMD-2 cells were transfected with miR-140-5p inhibitor or negative control (100 nM), the levels of MMD and phospho-Erk1/2 were measured by Western blotting.

4. Discussion

Lung cancer attracts more researchers' attention because of the high global mortality rate. Chen et al. [3] identified an RT-PCR–based five-gene signature (including DUSP6, MMD, STAT1, ERBB3, and LCK) using risk scores based on microarray and decision-tree analyses of tumor specimens from patients with NSCLC. The five genes may reveal targets for the development of therapy for lung cancer. Among the five genes, MMD attracted our attention because the exact biological function of MMD in cancer is not clear so far.

MMD was named because it was high expressed in mature macrophages but not in monocytes. However, recent studies show that MMD mRNA can be detected in almost all tissues [5]. On the other hand, MMD have exceptionally evolutionary rooting with substantially greater sequence similarity with the bacterial hemolysin III type protein, and the MMD protein sequence is high conserved in different species, sharing 99% amino acid sequence identity between the orthologue of human and mouse [4]. The deep evolutionary rooting and high conservation of MMD protein suggest that MMD probably plays an important role in cellular process. In this study, we demonstrate that the protein level of MMD is higher in lung cancer tissues compared with matched normal lung tissues (Fig. 1). Specifically, we found that knockdown of MMD promoted cell cycle arrest and inhibited the growth of A549 and LLC lung cancer cell lines (Fig. 2 and Fig. S1). Our results suggest that MMD likely plays an oncogene role.

MicroRNAs have recently been discovered as one of the crucial players in lung cancer through posttranscriptional regulation of tumor suppressors and oncogenes. Therefore, we wanted to know whether MMD is regulated by microRNAs. To screen out the possible upstream microRNAs, we used four different prediction algorithms to predict upstream microRNAs targeted for MMD. We gained the candidated microRNA, miR-140-5p, which has been indicated to be a possible tumor suppressor in human malignances, such as NSCLC and HCC [9–12]. In the present study, we demonstrated that MMD is a critical downstream target of miR-140-5p, and this conclusion is supported by the following evidence: (1) MMD was upregulated in NSCLC tissues and inversely correlated with the expression levels of miR-140-5p (Fig. 3A); (2) conserved complementary sequence of miR-140-5p is identified in the 3′ UTR of MMD mRNA (Fig. 3C and Fig. S2); (3) overexpression of miR-140-5p significantly reduced MMD protein levels in A549 cells (Fig. 3B), whereas inhibition of miR-140-5p enhanced MMD expression (Fig. 4C); (4) miR-140-5p overexpression reduced the activity of a luciferase reporter containing the wild-type 3′-UTR of MMD mRNA, but had no effect on the luciferase reporter containing the mutant MMD 3′-UTR (Fig. 3C); (5) the effect of miR-140-5p inhibition on A549 or LLC cell proliferation was reversed by knockdown of MMD (Fig. 3D and E, Fig. S3). Together, these data strongly suggest that miR-140-5p inhibits A549 or LLC lung cancer cell growth through downregulating MMD.

Recent evidence has confirmed that MMD is exclusively localized in Golgi apparatus but not the plasma membrane [5,13]. Then how does MMD affect cell proliferation in lung cancer cells? A new paradigm of spatial regulation of Ras signaling in Golgi apparatus by MMD has been uncovered. MMD can interact with Ras and enhance its retention and activity in Golgi apparatus, subsequently leading to sustained Erk signaling [13,14]. Moreover, a recent study in zebrafish provides a new piece of evidence that downregulation of Ras/ERK signaling can be caused by MMD knockdown [15]. Liu et al. [5] also has demonstrated that overexpression of MMD

increases Erk signaling in macrophages. Therefore, we detected the Erk signaling in our system. We found that the activation of Erk1/2 is higher in lung cancer tissues than the matched normal lung tissues (Fig. 4A). And in A549 cells knockdown of MMD could reduce the activation of Erk1/2 (Fig. 4B). Meanwhile, overexpression of miR-140-5p also impaired phosphorylated Erk1/2 (Fig. 4B). Whereas inhibition of miR-140-5p promoted the activation of Erk1/2 and this effect could be significantly blunted by knockdown of MMD (Fig. 4C). These data suggest that miR-140-5p/MMD axis likely affects the cell proliferation of lung cancer cells by regulating Erk signaling.

In conclusion, our study provides the first demonstration that the miR-140-5p/MMD/Erk cascade plays an important role in the growth of lung cancer cells. And our findings suggest that miR-140-5p/MMD axis could serve as new molecular targets for the therapy against lung cancer.

Acknowledgments

This work was supported by National Natural Science Foundation of China (Grant No. 81300325) and China Postdoctoral Science Foundation (Grant No. 2013M542440).

Appendix A. Supplementary data

Supplementary data associated with this article can be found, in the online version, at http://dx.doi.org/10.1016/j.bbrc.2014.06.075.

References

[1] J.R. Molina, P. Yang, S.D. Cassivi, S.E. Schild, A.A. Adjei, Non-small cell lung cancer: epidemiology, risk factors, treatment, and survivorship, Mayo Clin. Proc. 83 (2008) 584–594.
[2] A. Verdecchia, S. Francisci, H. Brenner, G. Gatta, A. Micheli, L. Mangone, et al., Recent cancer survival in Europe: a 2000–02 period analysis of EUROCARE-4 data, Lancet Oncol. 8 (2007) 784–796.
[3] H.Y. Chen, S.L. Yu, C.H. Chen, G.C. Chang, C.Y. Chen, A. Yuan, et al., A five-gene signature and clinical outcome in non-small-cell lung cancer, N. Engl. J. Med. 356 (2007) 11–20.
[4] M. Rehli, S.W. Krause, L. Schwarzfischer, M. Kreutz, R. Andreesen, Molecular cloning of a novel macrophage maturation-associated transcript encoding a protein with several potential transmembrane domains, Biochem. Biophys. Res. Commun. 217 (1995) 661–667.
[5] Q. Liu, J. Zheng, D.D. Yin, J. Xiang, F. He, Y.C. Wang, et al., Monocyte to macrophage differentiation-associated (MMD) positively regulates ERK and Akt activation and TNF-α and no production in macrophages, Mol. Biol. Rep. 39 (2012) 5643–5650.
[6] D.P. Bartel, MicroRNAs: genomics, biogenesis, mechanism, and function, Cell 116 (2004) 281–297.
[7] G.A. Calin, C.M. Croce, MicroRNA signatures in human cancers, Nat. Rev. Cancer 6 (2006) 857–866.
[8] S.I. Rothschild, Epigenetic therapy in lung cancer – Role of microRNAs, Front. Oncol. 3 (2013) 158.
[9] H. Yang, F. Fang, R. Chang, L. Yang, MicroRNA-140-5p suppresses tumor growth and metastasis by targeting transforming growth factor β receptor 1 and fibroblast growth factor 9 in hepatocellular carcinoma, Hepatology 58 (2013) 205–217.
[10] A. Takata, M. Otsuka, T. Yoshikawa, T. Kishikawa, Y. Hikiba, S. Obi, et al., MicroRNA-140 acts as a liver tumor suppressor by controlling NF-κB activity by directly targeting DNA methyltransferase 1 (Dnmt1) expression, Hepatology 57 (2013) 162–170.
[11] Y. Yuan, Y. Shen, L. Xue, H. Fan, MiR-140 suppresses tumor growth and metastasis of non-small cell lung cancer by targeting insulin-like growth factor 1 receptor, PLoS One 8 (2013) e73604.
[12] Y. Zhang, G. Eades, Y. Yao, Q. Li, Q. Zhou, Estrogen receptor α signaling regulates breast tumor-initiating cells by down-regulating miR-140 which targets the transcription factor SOX2, J. Biol. Chem. 287 (2012) 41514–41522.
[13] T. Jin, Q. Ding, H. Huang, D. Xu, Y. Jiang, B. Zhou, et al., PAQR10 and PAQR11 mediate Ras signaling in the Golgi apparatus, Cell Res. 22 (2012) 661–676.
[14] W. Peng, Q. Lei, Z. Jiang, Z. Hu, Characterization of Golgi scaffold proteins and their roles in compartmentalizing cell signaling, J. Mol. Histol. (2013). Epub ahead of print.
[15] H. Huang, T. Jin, J. He, Q. Ding, D. Xu, L. Wang, et al., Progesterone and adipoQ receptor 11 links ras signaling to cardiac development in zebrafish, Arterioscler. Thromb. Vasc. Biol. 32 (2012) 2158–2170.